THE JOURNAL OF PHYSICAL CHEMISTRY B

Article

pubs.acs.org/JPCB

Measurement and Control of pH in the Aqueous Interior of Reverse Micelles

Bryan S. Marques,[†] Nathaniel V. Nucci,[†] Igor Dodevski, Kristina W. C. Wang, Evangelia A. Athanasoula, Christine Jorge, and A. Joshua Wand*

Graduate Group in Biochemistry and Molecular Biophysics and Johnson Research Foundation and Department of Biochemistry and Biophysics, University of Pennsylvania Perelman School of Medicine, Philadelphia, Pennsylvania 19104-6059, United States

Supporting Information

ABSTRACT: The encapsulation of proteins and nucleic acids within the nanoscale water core of reverse micelles has been used for over 3 decades as a vehicle for a wide range of investigations including enzymology, the physical chemistry of confined spaces, protein and nucleic acid structural biology, and drug development and delivery. Unfortunately, the static and dynamical aspects of the distribution of water in solutions of reverse micelles complicate the measurement and interpretation of fundamental parameters such as pH. This is a severe disadvantage in the context of (bio)chemical reactions and protein structure and function, which are generally highly sensitive to pH. There is a need to more fully characterize and control the effective pH of the reverse micelle water core. The buffering effect of titratable head groups of the reverse micelle surfactants is found to often be the dominant variable defining the pH of the water core. Methods for measuring the pH of the reverse micelle aqueous interior using one-dimensional ^{1}H and two-dimensional heteronuclear NMR spectroscopy are described. Strategies for setting the effective pH of the reverse micelle water core are demonstrated. The exquisite sensitivity of encapsulated proteins to the surfactant, water content, and pH of the reverse micelle is also addressed. These results highlight the importance of assessing the structural fidelity of the encapsulated protein using multidimensional NMR before embarking upon a detailed structural and biophysical characterization.

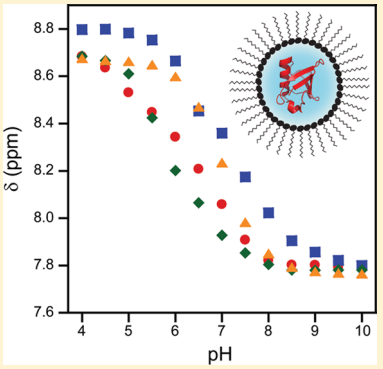

INTRODUCTION

Reverse micelles are nanoscale assemblies that spontaneously organize from mixtures of appropriate surfactant molecules, small volumes of polar solvent, and bulk nonpolar solvent. The polar, typically aqueous[1] interior of a reverse micelle provides a stable nanoscale confinement volume that has been used for decades in a wide variety of applications in synthetic, physical, and biological chemistry. Reverse micelles have been used for studies of nanoconfinement effects on water behavior,[2−4] protein structure[5−12] and biophysics,[13−16] enzymatic catalysis,[17] and nucleic acid structure and dynamics[18] and even used as a vehicle for drug delivery.[19] In recent years, reverse micelle encapsulation of proteins and nucleic acids has emerged as a particularly powerful tool for the study of macromolecular structure, function, and biophysics using high-resolution heteronuclear NMR spectroscopy.[20−22]

The adaptation of reverse micelle encapsulation for high-resolution solution NMR spectroscopy of biological macromolecules was originally undertaken to overcome the deleterious effects of their slow molecular reorientation. Single protein molecules encapsulated within the aqueous core of reverse micelles dissolved in low viscosity fluids can thus be made to tumble faster than they would by themselves in aqueous solution.[20] Faster molecular reorientation leads to more optimal NMR relaxation properties and improved performance. In the context of structural biology and biophysics, the homogeneity and fidelity of encapsulation become critical and largely define the utility of this approach. In the context of high-resolution NMR of encapsulated proteins, small spherical reverse micelles containing a single protein molecule can be prepared with appropriate surfactant mixtures under water-limited conditions in short-chain alkane solvents including propane[20] and ethane.[21,22]

Over the past decade there has been a renewed interest in expanding the library of surfactant systems that can support encapsulation of proteins with a range of properties such as isoelectric point, size, oligomerization state, and the presence of bound ligands or cofactors. The classic anionic surfactant bis(2-ethylhexyl)sulfosuccinate (AOT) has proven to be poor in this regard.[22] Appropriate mixtures of amphiphilic surfactants such as cetyltrimethylammonium bromide (CTAB), dodecyltrimethylammonium bromide (DTAB), lauryldimethylamine oxide (LDAO), and decylmonoacylglycerol (10MAG) and cosurfactants such as hexanol form small homogeneous reverse micelles in the low viscosity short-chain alkanes and have proven to be quite successful in the encapsulation of proteins and nucleic acids with high structural fidelity.[9,22−25]

Received: October 18, 2013
Revised: January 26, 2014
Published: February 7, 2014

   dx.doi.org/10.1021/jp4103349 | J. Phys. Chem. B 2014, 118, 2020−2031

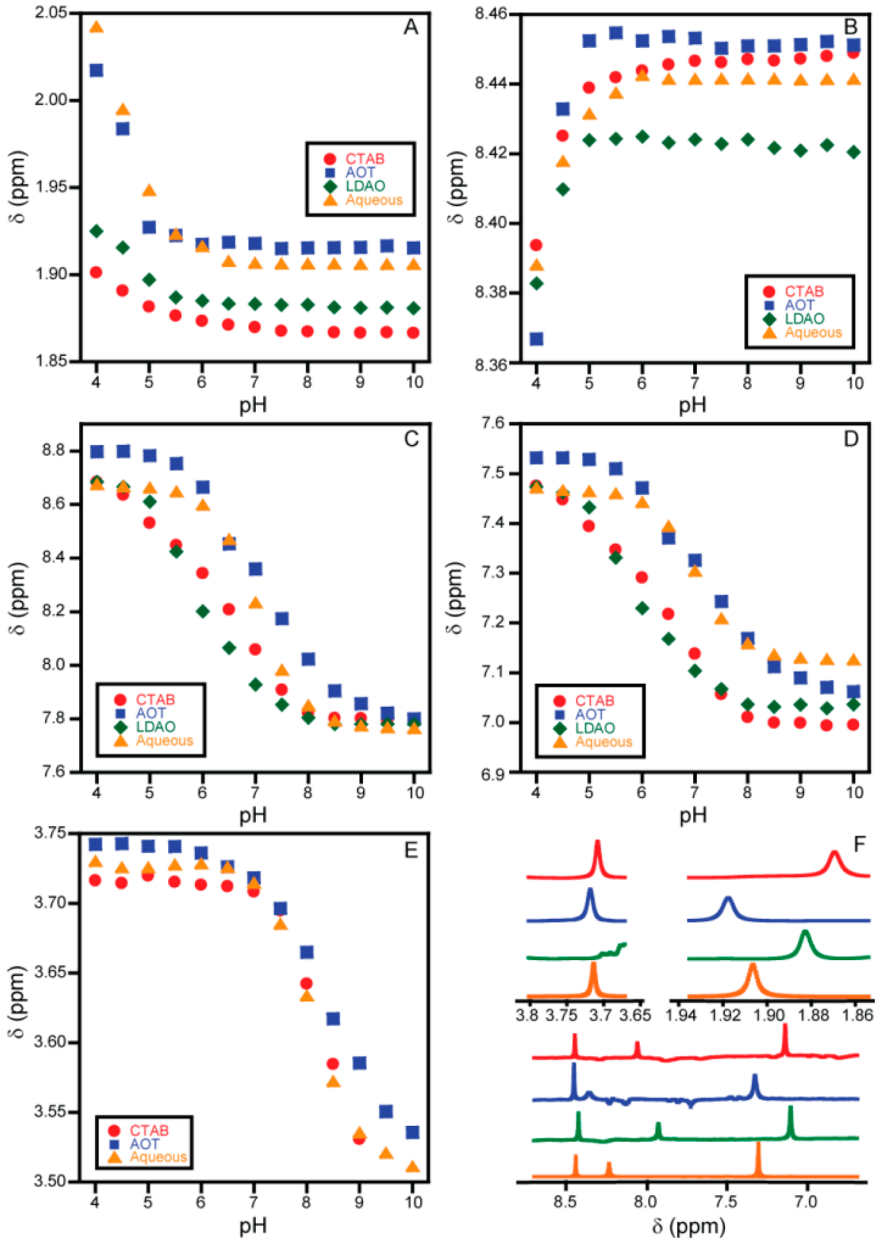

Figure 1. Buffer chemical shifts as a function of target pH in aqueous solution and reverse micelles composed of various surfactant mixtures. The pH-dependent chemical shifts of buffer hydrogen atoms[40,41] are shown: (A) acetate; (B) formate; (C, D) imidazole H2 and H4/5, respectively; (E) Tris. Data are shown for aqueous buffer samples (orange triangles) and in the three reverse micelle surfactant conditions tested: AOT (blue squares), CTAB/hexanol (red circles), and 10MAG/LDAO (green diamonds). In all cases except CTAB/hexanol, the surfactants were pre-equilibrated with solutions at the target pH (see text). The signal for Tris overlaps significantly with surfactant peaks in the 10MAG/LDAO mixture and was therefore omitted from these data. Representative spectra of each buffer molecule in each environment at pH 7 are depicted in (F) using the same color scheme with the upper left spectra corresponding to Tris, the upper right corresponding to acetate, and the lower spectra corresponding to both formate (left peak in all spectra) and imidazole chemical shifts.

A critical parameter for any chemical application but particularly in the context of protein biochemistry and biophysics is the pH of the reverse micelle aqueous core. The concept of pH in the reverse micelle water pool presents a somewhat complicated situation.[26,27] The measurement and meaning of pH in reverse micelles is complicated by the potential for interactions between the buffers of the water pool and the surfactants and by the possibility of an inhomogeneous distribution within the water core.[28,29] A number of studies have been undertaken to experimentally characterize pH within reverse micelle water cores including the use of oxovanadate probes with ^{51}V NMR,[27,30−33] phosphate and pyrophosphate with ^{31}P NMR,[29,34] measurements of water T_2 relaxation times with proton NMR,[35] and hydroxypyrene trisulfonate and fluorescein measurements using optical spectroscopy.[26,36]

Here we focus on the view of pH provided by solution NMR spectroscopy of reverse micelles where dynamical effects can be particularly important to consider. Unlike many other types of spectroscopy, NMR parameters such as the chemical shift can be averaged by relatively slow processes on the order of milliseconds or faster. This is an important consideration in the context of pH where the number of waters in a typical single reverse micelle core is insufficient to present, on average, even a single hydronium or hydroxide ion. As a result, the

dx.doi.org/10.1021/jp4103349 | J. Phys. Chem. B 2014, 118, 2020−2031

instantaneous "pH" in the core of an individual reverse micelle may vary widely. Importantly, however, reverse micelles dissolved in liquid alkane solvents collide and exchange water cores on the microsecond time scale.[37−39] These exchange events lead to averaging of ionization states on the chemical shift time scale such that a single average spectrum is generally obtained. This averaged spectrum offers an assessment of the overall or effective pH of the ensemble of reverse micelles in a particular solution.

In this study we implement in the context of the reverse micelle aqueous core a method that has been previously established for pH monitoring in bulk aqueous solution, namely, observation of ^{1}H NMR signals of common, unlabeled buffer molecules.[40,41] The approach is validated by reference to the corresponding pH dependence of amide ^{1}H and ^{15}N resonances of an encapsulated protein. It is found that the titratable surfactant molecules can dominate the effective pH of the water core and generally overwhelm the buffering contributions of molecules in the aqueous core. Methods are described to set the effective pH of the reverse micelle water pool when a reverse micelle sample is prepared and to adjust the pH after sample preparation. Importantly, it is shown that the structural fidelity of an encapsulated protein is often exquisitely sensitive to the reverse micelle conditions, including the effective pH. It is highly recommended that the structural integrity of encapsulated proteins be directly characterized using multidimensional NMR spectroscopy rather than interrogated with less comprehensive methods such as UV/visible absorbance or fluorescence emission spectroscopy.

MATERIALS AND METHODS

"Empty" Reverse Micelle Sample Preparation. All protein-free or "empty" reverse micelle samples were prepared by mixing appropriate amounts of surfactant in a 50/50 (v/v) mixture of pentane/*d*-pentane (d-12) (Cambridge Isotopes, Cambridge, MA) followed by injection of an appropriate volume of the desired aqueous buffer solution except samples at pH 7 which were prepared in 100% *d*-pentane for collection of spectra for Figure 1. Three surfactant mixtures were used: 75 mM cetyltrimethylammonium bromide (CTAB) with 450 mM hexanol as cosurfactant, 75 mM bis(2-ethylhexyl)sulfosuccinate (AOT), and a mixture of 22.5 mM lauryldimethylamine *N*-oxide (LDAO) and 52.5 mM decylmonoacylglycerol (10MAG). All buffers were 25 mM prepared to the stated bulk pH. The volume of buffer used for reverse micelle samples defines the molar ratio of water to total surfactant concentration (also known as "water loading" and designated as W_0). For protein-free samples, a target W_0 of 15 was used for all mixtures. 10MAG/LDAO mixtures had a final W_0 of 12, as measured by NMR integration of the ^{1}H spectra. AOT and CTAB samples had a final W_0 of 15. 10MAG/LDAO reverse micelles containing imidazole only were also tested at W_0 of 20 to examine the W_0 dependence of buffer response. All unlabeled chemicals were purchased from Sigma-Aldrich (St. Louis, MO) except LDAO (Affymetrix, Santa Clara, CA).

Characterization of Surfactant pK_a Values. To characterize the buffering capacity of the surfactant headgroups, each surfactant (AOT, CTAB, LDAO, and 10MAG) was individually dissolved (1−2 mM) in water (with 12% ethanol required to solubilize 10MAG) and titrated with 1 M HCl or 1 M NaOH over a pH range from 4 to 10. The pH of all aqueous solutions was monitored with an Accumet AB15+ Basic pH meter and electrode (Fisher Scientific, Pittsburgh, PA).

pH and W_0 Adjustment of the Reverse Micelle Core. The pH of the water cores of reverse micelles was adjusted in two ways. In one approach, samples were prepared using surfactants as supplied without further purification or manipulation. CTAB/hexanol reverse micelles prepared with aqueous buffer cores showed pH values within 0.5 pH units of the aqueous buffer (see below for measurement methods), indicating that this surfactant mixture does not contribute appreciable buffering capacity in the pH 4−10 range. In contrast, AOT and 10MAG/LDAO reverse micelles yielded pH values of 5−5.5 and 7−7.5, respectively, *regardless of the pH of the injected buffer solution*, indicating that these surfactants have significant buffering capacity. The pH of these samples can be adjusted post facto by the direct addition of the appropriate amount of HCl or NaOH. After addition of a small volume of acid or base, the solution was slowly inverted, vortexed for 5−10 s, and allowed to equilibrate without agitation for 5 min before data collection. The pH of the aqueous nanopool was monitored with one-dimensional ^{1}H NMR. During this pH adjustment, the W_0 often increased by 4 or 5. In order to lower the W_0, the pentane and some of the water in the reverse micelle solution were evaporated by introducing low pressure N_2 gas. The solution was allowed to evaporate to approximately half of the total volume of the sample and then returned to the full volume with *d*-pentane. Depending on the total volume of the sample, this procedure lowered W_0 by approximately 2 or 3. It should be noted that this procedure, termed the injection−evaporation method, need not have any impact on the encapsulated protein.[23]

The second approach for adjustment of the pH in the reverse micelle core involved preadjustment of the pH of the AOT and LDAO headgroups prior to reverse micelle sample preparation as follows. AOT was dissolved in water (1 mg/mL), titrated to the target pH, and lyophilized. This procedure was repeated until the lyophilized AOT gave a consistent pH when redissolved in water. Generally three to four rounds of adjustment and lyophilization were required. Note that the appearance of the dried AOT varied with pH: AOT at higher pH (8−10) had a more coarse-grained appearance than the typical pasty appearance of AOT at lower pH. The number, positions, and splitting of the AOT ^{1}H NMR signals did not change with titration, confirming that the AOT was chemically unaltered by this pH adjustment. In order to preadjust the pH of the LDAO headgroup, the appropriate amounts of LDAO and 10MAG for each sample were dissolved in a solution of 12% ethanol, titrated to the correct pH, and then lyophilized. Though LDAO is freely soluble in aqueous solution, 10MAG requires 12% ethanol to solubilize so that these surfactants could be premixed at the appropriate pH. A single round of adjustment and lyophilization was sufficient for the 10MAG/LDAO mixture at all pH values tested. These surfactants were then used for reverse micelle sample preparation as outlined above.

Protein Purification and Encapsulation. Uniformly ^{15}N-labeled human ubiquitin (8.5 kDa), oxidized horse cytochrome c (11.4 kDa), and the L99A mutant of lysozyme from the bacteriophage T4 virus (18.6 kDa) were prepared as previously described ($^{15}NH_4Cl$ from Cambridge Isotopes).[25,42−44] Ubiquitin-containing reverse micelle samples were prepared as follows. For each sample, 2 mg (hereafter referred to as one aliquot) of dried ubiquitin was dissolved in 1 mL of water. The pH of this protein solution was adjusted to the target pH using dilute (0.1 or 0.01 M) HCl or NaOH; the sample was then

dx.doi.org/10.1021/jp4103349 | J. Phys. Chem. B 2014, 118, 2020−2031

lyophilized. This preadjustment of the protein's pH prior to encapsulation is essential for preparation of reverse micelle samples wherein the protein structural integrity is preserved and the target pH is obtained. The dried protein was then dissolved in the appropriate volume of buffer for a target W_0 of 10. The same adjustment of the protein pH may be achieved via dialysis or buffer exchange methods followed by concentration of the protein sample to the appropriate volume for encapsulation. The same buffer mix and preparation method as described above for protein-free samples were used for ubiquitin-containing reverse micelle samples.

To illustrate the buffering capacity of the AOT and 10MAG/LDAO mixtures, one aliquot of ubiquitin at pH 5 was encapsulated in unadjusted 10MAG/LDAO, and one aliquot of ubiquitin at pH 7 was encapsulated in unadjusted AOT. In order to demonstrate the preparation of an encapsulated protein sample at a target pH, three samples were prepared with a final protein concentration of 150 μM and a W_0 of 10 using ubiquitin and 10MAG/LDAO that had been preadjusted to pH 5, 7, or 9. These samples were prepared with the addition of 24 mM hexanol as cosurfactant.[23] In order to demonstrate the ability to further adjust the pH of protein samples after encapsulation, the pH 5 ubiquitin sample was titrated to pH 7 and pH 9 using the methods described above for protein-free reverse micelles, and a ^{15}N HSQC spectrum was recorded at each pH. Likewise, the pH 7 sample was titrated to pH 5 and a ^{15}N HSQC spectrum was recorded.

Cytochrome *c* was used to demonstrate the degree of protein foldedness in reverse micelles detected using NMR and optical spectroscopy. Cytochrome *c* (6 mM aqueous solution) was encapsulated in preadjusted 10MAG/LDAO as described above at a W_0 of 15 and a pH of 5 to a final protein concentration of 140 μM. Cytochrome *c* was also encapsulated in 75 mM AOT at the same pH and protein concentration. Aqueous cytochrome *c* was prepared in 50 mM sodium acetate at pH 5 with 50 mM NaCl. The pH of the aqueous cytochrome *c* sample was adjusted to 2.5 by direct addition of HCl using a standard pH meter for measurement. The cytochrome *c* in 10MAG/LDAO reverse micelles was unfolded by titration of the sample through direct addition of an appropriate volume of 6 M HCl to a pH of ~2.5, as determined by the ^{1}H NMR position of the acetate peak. It should be noted that that stability of this sample was limited (~2 h) because of the extremely low pH.

The L99A mutant of T4 lysozyme was used to monitor protein foldedness in reverse micelles with changing pH and W_0 detected using NMR and tryptophan fluorescence emission spectroscopy. Aqueous T4 lysozyme (5 mM) was prepared in 50 mM sodium acetate at pH 5 with 50 mM NaCl. The protein was then encapsulated in a 75 mM surfactant mixture containing 10MAG, LDAO, and DTAB in a molar ratio of 70:20:10 that had been preadjusted to a pH of 5. In order to monitor the effect of pH on protein foldedness, T4 lysozyme was encapsulated at pH 5 at a W_0 of 18. The pH was then adjusted to 3.5 and 2.5 by direct injection of concentrated HCl and monitored by 1D proton NMR as described above. In order to maintain a constant W_0, the injection−evaporation method was used as described above. To monitor the effect of water loading on protein foldedness, T4 lysozyme was initially encapsulated at pH 5 with a W_0 of 12 at a final protein concentration of 80 μM. The W_0 of the sample was raised to 18 by direct injection of the proper amount of buffer followed by slow inversion and vortexing for 5−10 s. All mixtures were allowed to equilibrate without agitation for 30 min before data collection.

Optical and Fluorescence Spectroscopies. Optical spectroscopy on cytochrome *c* was used to observe changes in the absorption of the Soret band upon changing pH. All optical spectra were collected from 200 to 800 nm on a Cary 50 Bio UV−visible spectrophotometer (Varian/Agilent Technology, Santa Clara, CA). All aqueous spectra were baseline-corrected against buffer, while all reverse micelle spectra were baseline-corrected against pentane. The optical absorbance graphs were created with Kaleidagraph (Synergy Software, Reading, PA).

Fluorescence emission spectroscopy on T4 lysozyme (L99A) was used to examine native tryptophan fluorescence of the encapsulated protein as water loading increased and pH decreased. An excitation wavelength of 297 nm was used for aqueous protein samples while a wavelength of 291 was used for reverse micelle samples. These were the wavelengths of maximum excitation for the samples, respectively. All emission spectra were collected on a Horiba Jobin Yvon (Edison, NJ) Fluorolog-3 from 310 to 500 nm with excitation and emission slit widths of 4 and 1 nm, respectively. Normalized emission spectra were created with Kaleidagraph.

NMR Spectroscopy. NMR data were collected at 25 °C at 500 or 600 MHz (^{1}H) on Bruker AVANCE III spectrometers equipped with TXI cryoprobes. Buffer molecule chemical shifts were determined using 1D ^{1}H NMR spectra with a selective presaturation pulse centered at the methyl region of the protonated pentane (~2 ppm) to suppress signal from the alkane solvent. Presaturation was not used for samples in 100% *d*-pentane. ^{1}H spectra were collected using 256 scans, which was required due to the relatively low effective concentration of buffer molecules in the reverse micelle samples (500 μM each as compared to 75 mM surfactant). ^{15}N HSQC spectra of encapsulated ubiquitin and T4 lysozyme L99A mutant (for the W_0 titration study) were collected with 64 and 100 complex increments, respectively, at 500 MHz. Spectra of encapsulated cytochrome *c* and T4 lysozyme L99A mutant (for the pH titration study) were collected at 600 MHz with 48 and 100 complex increments, respectively. The cytochrome *c* spectra were linear-predicted to 64 complex increments. The free (bulk) aqueous protein ^{15}N HSQC spectra for ubiquitin and cytochrome *c* were collected with 4 scans, while the reverse micelle spectra were collected with 8 scans. The aqueous spectra for T4 lysozyme L99A mutant were collected with 16 scans, while the reverse micelle spectra were collected with 32 scans except for the reverse micelle sample at pH 2.5, which was collected with 128 scans due to diminished signal-to-noise. One-dimensional ^{1}H spectra were referenced to dimethylsilapentanesulfonate (DSS, Sigma)[45] and processed using Topspin 3.0. All ^{15}N HSQC spectra were processed using ALNMR.[46] Graphs of chemical shifts and fitting of pH-dependent chemical shift data were performed with Kaleidagraph.

RESULTS AND DISCUSSION

Monitoring pH in Reverse Micelles. The pH of the aqueous core encapsulated within a reverse micelle is a complex property of these systems.[26,27,47] Despite its complexity and importance, this property of reverse micelle samples is frequently overlooked under the assumption that the aqueous solution used to prepare a reverse micelle mixture determines the pH of the encapsulated aqueous core. However, in

dx.doi.org/10.1021/jp4103349 | J. Phys. Chem. B 2014, 118, 2020−2031

principle, the most abundant component that can contribute to the internal pH of the encapsulated solution in any reverse micelle mixture is titratable surfactant molecules, which are typically 1−2 orders of magnitude higher in concentration than the buffer or macromolecular components of the reverse micelle mixture.[34]

Reverse micelles prepared in liquid alkanes and used in structural biology and biophysics have historically comprised various mixtures of the anionic AOT, cationic CTAB and its variants, and neutral surfactants such as hexanol and various polyethers. More recently, a new surfactant mixture based on the zwitterionic LDAO and the uncharged 10MAG has been described.[23] To examine the buffering capacity of the AOT, CTAB, LDAO, and 10MAG headgroups, each was dissolved in water (with 12% ethanol for 10MAG) and titrated over a pH range from 4 to 10. As expected, CTAB and 10MAG were found to have no buffering capacity in this pH range while both AOT and LDAO have apparent pK_a values in the range of 3−4. Aqueous solutions of AOT had an initial pH of 5 to 5.5, regardless of the manufacturer lot number. Aqueous LDAO solutions showed a broader initial pH range of 6.5 to 8, depending on which manufacturer batch was used. From these tests, it was determined that both AOT and LDAO should have dominant buffering capacity in the reverse micelle mixture. While measurement of pH in bulk aqueous solution is simple, measurement of the pH of the reverse micelle core is much more difficult.

Previous efforts to measure the pH in reverse micelles have often used either colorimetric pH indicators or pH-dependent fluorophores. Optical probes, where the time scale of the reporting phenomenon is quite short, can be tricky to interpret because of superpositions of spectra due to subtle pH gradients within the reverse micelle interior and the propensity for these amphiphilic molecules to partition into varying regions of the reverse micelle mixture.[27] From the point of view of NMR spectroscopy of macromolecules, relatively long time scale processes (i.e., millisecond) can result in chemical shift averaging, and it is this average that captures information about the structural integrity of encapsulated proteins by reference to their spectra in bulk aqueous solution. The small size of the water core of an individual reverse micelle (approximately 10^3 water molecules) means that at neutral pH only about one in a million reverse micelles actually carries a hydronium ion. However, under most conditions, the frequent collision of reverse micelle particles results in complete averaging of ionization states of the encapsulated protein and other titratable molecules. The pH-dependence of ^{1}H NMR resonances of buffer molecules has been shown previously to provide a rapid and precise measure of the pH in bulk aqueous solution.[40,41] In order to be useful as a pH indicator in the context of the reverse micelle water core, buffer molecules should provide resolved reporter ^{1}H resonances that do not interfere with the assessment of other parameters of reverse micelle solutions such as the determination of water loading by integration of water and surfactant resonances. They should also not interact significantly with the reverse micelle surfactant shell. Four of the buffers used for pH determination in bulk solution were identified to satisfy these criteria: imidazole, Tris, formate, and acetate. These span a useful pH range of 4−10.[40,41] Imidazole (pK_a ≈ 7), which provides an effective pH indicator range of approximately 5.5−8, contains three hydrogens whose chemical shifts change as a function of pH. Imidazole H2 has a chemical shift range of 7.7−8.7 ppm while the two degenerate H4/5 hydrogens have a chemical shift range of 7.1−7.5 ppm. Tris (pK_a ≈ 8) provides an effective pH indicator range of 6.5−10 and a chemical shift range of 3.5−3.75 ppm. Formate (pK_a ≈ 3.8) provides an effective pH indicator range of 4.0−5.5 and a chemical shift range of 8.38−8.45 ppm. Acetate (pK_a ≈ 4.75) has an effective pH range of 4.0−6.5 and a chemical shift range of 1.90−2.05 ppm. The main impediment to using this approach in reverse micelles is the low effective concentration of the buffer molecules in the sample relative to the surfactant molecules and solvent whose NMR signals can bleed into the signal of the buffer chemical shifts. Deuterated solvents and the usual solvent suppression techniques[48] can be used to mitigate interference from solvent signals.

Initial experiments were performed to investigate the presence of interactions between buffer molecules and the surfactants used here. ^{1}H NMR spectra of aqueous solutions containing each buffer at 25 mM with 25 mM DSS as a chemical shift reference were recorded in the presence and absence of small amounts (∼1 mM) of each of the three water-soluble surfactants used (AOT, CTAB, and LDAO) over the full pH range from 4 to 10 in increments of 0.5. These experiments confirmed that with small amounts of surfactant present there were no discernible pK_a shifts for any of the buffer molecules and only minute changes (<0.05 ppm) in buffer chemical shifts. This result was interpreted as indicating the absence of strong interactions between the surfactants and buffer molecules used here. The effects of the three surfactant mixtures (AOT, CTAB/hexanol, 10MAG/LDAO) on the pH of the reverse micelle water core were examined using samples prepared with the surfactants as provided by the manufacturers (i.e., without further purification or manipulation). Thirteen samples for each surfactant mixture were prepared by injecting the buffer mixture prepared at 0.5 pH increments from pH 4 to pH 10. ^{1}H NMR spectra of these samples showed that the pH of all AOT samples were within 0.5 units of pH 5 while all 10MAG/LDAO samples showed an aqueous nanopool pH within 0.5 units of pH 7.5. In contrast, CTAB/hexanol samples showed a simple titration curve without the need for pre-equilibration (Figure 1), showing that CTAB has negligible buffering capacity in the reverse micelle mixture over the pH range examined here. These results confirm that the protonation state of the AOT and LDAO headgroups dominate the pH of the reverse micelle when these surfactant mixtures are employed. To prepare samples in AOT or 10MAG/LDAO at a given target pH, the surfactants were pre-equilibrated to the target pH value (see Materials and Methods). Samples were prepared in this way for the 13 pH values described above and examined by ^{1}H NMR. The chemical shifts of the buffer molecules as a function of reverse micelle sample pH along with example spectra obtained at pH 7.0 are shown in Figure 1.

These data are shown based on the target pH, a view that illustrates some inconsistencies (RM vs aqueous) in the measured pH within the reverse micelle sample depending on which buffer was used to establish the pH (Figure 1). This is traced to a change in the effective pK_a and shows that some of the buffers interact with or are otherwise perturbed by the reverse micelle surfactants. Note that not all buffer molecules are appropriate for all surfactant mixtures. The pH-dependent hydrogen signal of Tris, for example, overlaps with a signal from AOT at high pH and overlaps significantly with one of the LDAO signals at all pH values (Figure 1F). These data indicate that there is not necessarily a particular buffer that will be ideal

for monitoring pH in all reverse micelle surfactant mixtures. However, a mixture of acetate and imidazole offers general applicability over a wide range of pH values (4−8.5).

Clearly the pH indicator molecules may experience a shift in their apparent pK_a values by as much as 1 pH unit upon encapsulation in some surfactant mixtures. For example, in the imidazole plots (Figure 1C,D), the chemical shifts of the AOT-encapsulated buffer appear to closely match those seen in aqueous solution while in the 10MAG/LDAO and CTAB/hexanol mixtures the chemical shifts seem to show a reduction in the pK_a from 7 to approximately 6.2. Comparison of the pH response of imidazole to that of Tris (Figure 1E) in the CTAB/hexanol mixture yields a conflicting result; i.e., one or more of the pH indicator molecules have experienced a shift in pK_a as a result of encapsulation.

To more quantitatively assess the apparent pK_a shifts for imidazole, the data were fit to eq 1,[41]

$$\mathrm{pH} = \mathrm{p}K_a - \log\left(\frac{\delta_{obs} - \delta_{HA}}{\delta_A - \delta_{obs}}\right) \quad (1)$$

where δ_A and δ_{HA} are the chemical shifts of the basic and acidic forms of the buffer, respectively, and δ_{obs} is the observed buffer chemical shift in a given sample. The data were fit using the target pH as the known quantity to determine an apparent pK_a for each solution condition (Table 1). On the basis of these data alone, the assumption that the sample is at the target pH is unfounded but the data from encapsulated proteins confirm the validity of this assumption (see below).

Table 1. Effective pK_a of Imidazole in Various Reverse Micelles

sample condition	imidazole (H2)	imidazole (H4/5)
aqueous	6.96	6.98
AOT (W_0 = 15)	7.29	7.30
CTAB (W_0 = 15)	6.22	6.21
10MAG/LDAO (W_0 = 12)	6.14	6.16
10MAG/LDAO (W_0 = 20)	6.72	6.79

The pK_a of imidazole varies by as much as 0.9 pH units across the various reverse micelle surfactant mixtures examined. The pK_a is also influenced by the water loading in the 10MAG/LDAO surfactant system. The sensitivity of the apparent pK_a of the indicator buffers requires that the pH-dependent response must first be characterized for each surfactant mixture.

Surfactant Molecules Dominate the pH of Reverse Micelles. The chemical shifts of proteins are well-known to exhibit exquisite sensitivity to pH. The amide nitrogen and amide hydrogen chemical shifts of the 8.5 kDa protein ubiquitin were used as indicators of the pH environment in the reverse micelle core. Ubiquitin was chosen as the protein indicator for these studies because of its stability over a wide pH range and its previously characterized amenability to encapsulation in many different surfactant mixtures.[9,22,49] Ubiquitin was prepared in aqueous solution at pH 5 or pH 7, and ^{15}N HSQC spectra were recorded (Figure 2A and Figure 2C, respectively). These spectra show the typical degree of pH-dependent chemical shift changes for proteins in aqueous solution. The aqueous protein sample at pH 5 was then encapsulated in 10MAG/LDAO, while the aqueous sample at pH 7 was encapsulated in AOT, both without preadjustment of the surfactant pH. ^{15}N HSQC spectra were collected for both

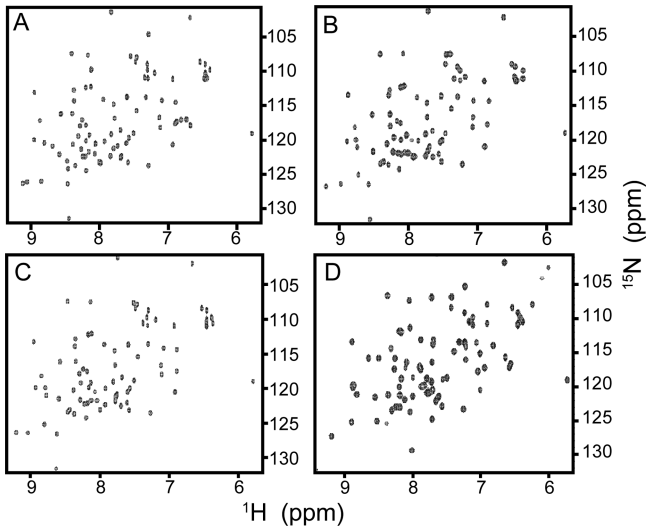

Figure 2. ^{15}N HSQC spectra of uniformly ^{15}N-labeled ubiquitin in aqueous solution at different pH and in various reverse micelle mixtures. Aqueous ubiquitin at pH 5 (A) was encapsulated in 10MAG/LDAO reverse micelles without prior pH equilibration of the surfactants. (B) Similarly, aqueous ubiquitin at pH 7 (C) was encapsulated in AOT without prior pH equilibration of the surfactant (D).

of these reverse micelle samples (Figure 2B and Figure 2D, respectively.) As described above, the chemical shifts of the buffer molecules in these samples indicated that the injected solution of ubiquitin, initially at pH 7, shifted to pH ≈ 5 upon encapsulation in unadjusted AOT. The protein ^{15}N HSQC spectrum agrees with this result. Indeed, this spectrum matches the previously determined assignments of encapsulated ubiquitin at pH 5.[9] By the same token, the buffer chemical shifts of ubiquitin solution, initially set to pH 5 and then encapsulated in unadjusted 10MAG/LDAO (2B), indicate that the aqueous core of the reverse micelle was at pH 7. The chemical shifts of the encapsulated ubiquitin closely match those of the aqueous pH 7 spectrum (2A). From these data, it is clear that the surfactant dominates the pH of the aqueous nanopool for reverse micelle mixtures composed of surfactants with titratable headgroups even in the presence of macromolecules.

Calibration of the Reverse Micelle Interior for Encapsulation of Proteins. The goal of this work was to establish a method by which reverse micelles could be prepared at a target pH or adjusted to a target pH after formation of the reverse micelle mixture. Both encapsulated ubiquitin and the chemical shifts of the four buffer molecules indicate clearly that the pH of the encapsulated solution is dominated by the protonation state of the AOT or 10MAG/LDAO surfactants prior to sample preparation. The ^{15}N HSQC spectrum of encapsulated ubiquitin was used to determine whether pre-equilibration of surfactants with an aqueous solution set at a target pH could be used to effectively set the effective pH of the reverse micelle core.

Ubiquitin was prepared in aqueous solution with a mixture of the four buffer pH indicators at three pH values: 5, 7, and 9. ^{15}N HSQC spectra were taken for each sample to have a reference spectrum of the aqueous protein to compare to the reverse micelle-encapsulated counterparts (Figure 3). These protein samples were then encapsulated in 10MAG/LDAO reverse micelles. 10MAG/LDAO was chosen for these tests

dx.doi.org/10.1021/jp4103349 | J. Phys. Chem. B 2014, 118, 2020−2031

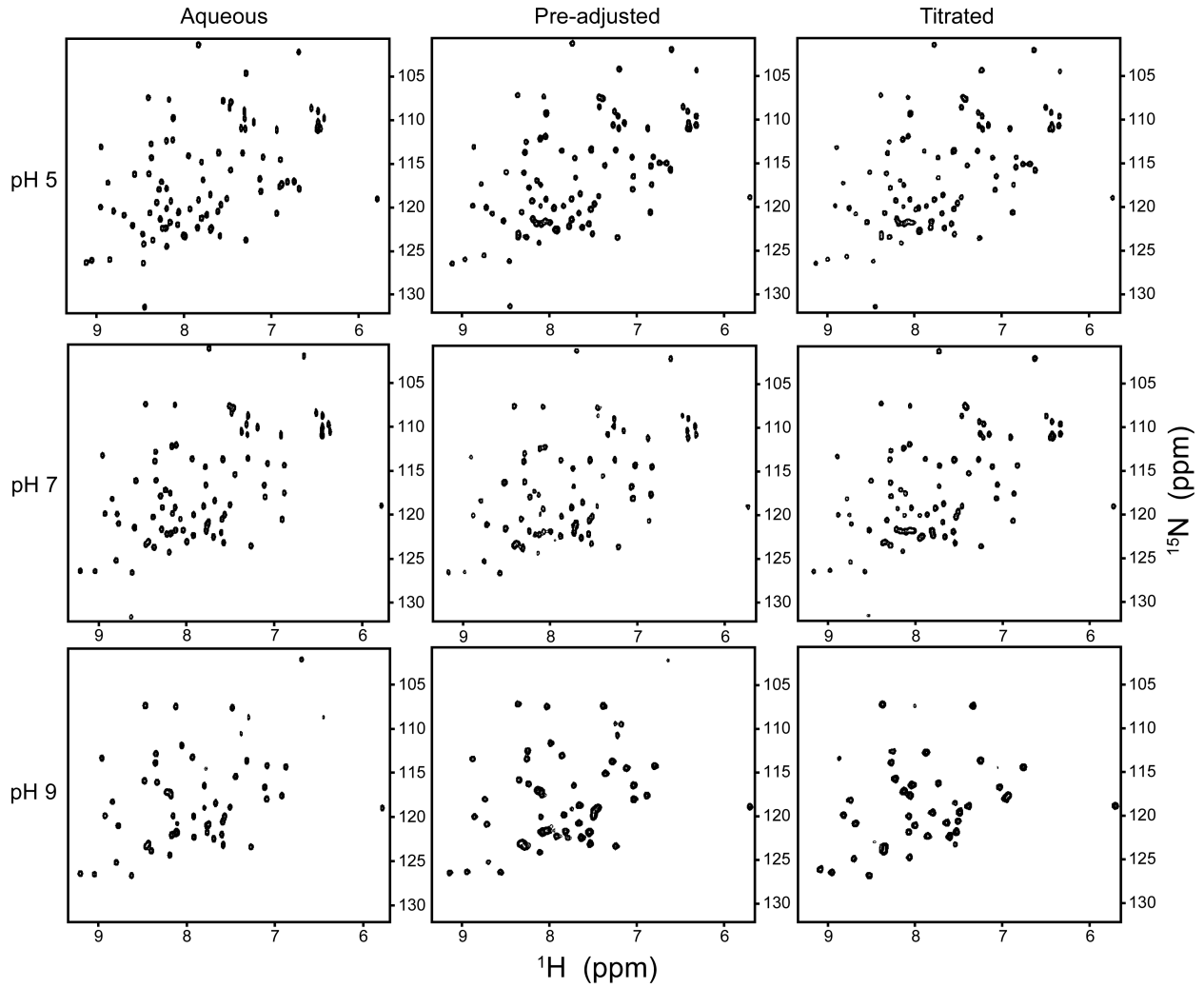

Figure 3. ^{15}N HSQC spectra of uniformly ^{15}N-labeled ubiquitin in aqueous solution at different pH and in 10MAG/LDAO reverse micelle mixtures pre-equilibrated to a given pH and after titration. Aqueous ubiquitin samples (left column) at the indicated pH were encapsulated in10MAG/LDAO to a W_0 of 10 that had been pre-equilibrated to the same pH (middle column). The preadjusted pH 9 reverse micelle sample was titrated to pH 7, then to pH 5. The preadjusted pH 7 reverse micelle sample was titrated to pH 9. The pH was monitored by tracking the chemical shift changes of the imidazole and acetate buffers in the solution.

because of its capacity to reproduce the aqueous chemical shifts of proteins upon encapsulation and its applicability to a wide variety of proteins over a broad pH range.[23] The surfactants had been pre-equilibrated to pH 5, 7 and 9, respectively, as described in Materials and Methods. The corresponding ^{1}H NMR spectra showed buffer resonance chemical shifts that closely matched those of the preadjusted protein-free samples (see Figure 1). The corresponding ^{15}N HSQC spectra (Figure 3) showed excellent agreement with the aqueous spectra, indicating that the effective pH of the reverse micelle water core had been set to the desired target. Thus, the shift of the pK_a of imidazole is due to encapsulation in 10MAG/LDAO and the titration curves shown in Figure 1 can be used for calibration of the internal pH of 10MAG/LDAO reverse micelles.

To test the utility of the buffer chemical shifts for measurement and adjustment of the reverse micelle pH, the pre-equilibrated reverse micelle samples were titrated to a different target pH by direct addition of concentrated acid or base while maintaining the W_0 of the sample (see Materials and Methods for details). These titrations were monitored using only the ^{1}H NMR signals of the imidazole and acetate buffers. Once the target pH was reached, a ^{15}N HSQC spectrum was collected (Figure 3, right column). The spectra of the titrated samples closely match those of both the pre-equilibrated and aqueous samples, confirming the utility of the internal buffer signals for measurement and adjustment of the pH of the reverse micelle core.

Composition and pH of the Reverse Micelle Can Affect Protein Stability. Whether or not a protein remains in its native conformation upon encapsulation is dependent on many factors including the composition of the surfactant mixture, the water loading, and the pH.[15,22,49] Despite the wealth of studies on proteins encapsulated in reverse micelles, efforts to discern the structural fidelity of the encapsulated protein vary widely.[6,17] Often no detailed examination of the conformational state of the encapsulated protein is undertaken, and if considered, only low-resolution methods such as optical spectroscopy or circular dichroism have been used.[5−8,17]

The vast majority of previous studies on encapsulated proteins have used AOT as the reverse micelle surfactant system. As we have demonstrated before[22] and show again here, AOT reverse micelles can frequently solubilize proteins

dx.doi.org/10.1021/jp4103349 | J. Phys. Chem. B 2014, 118, 2020−2031

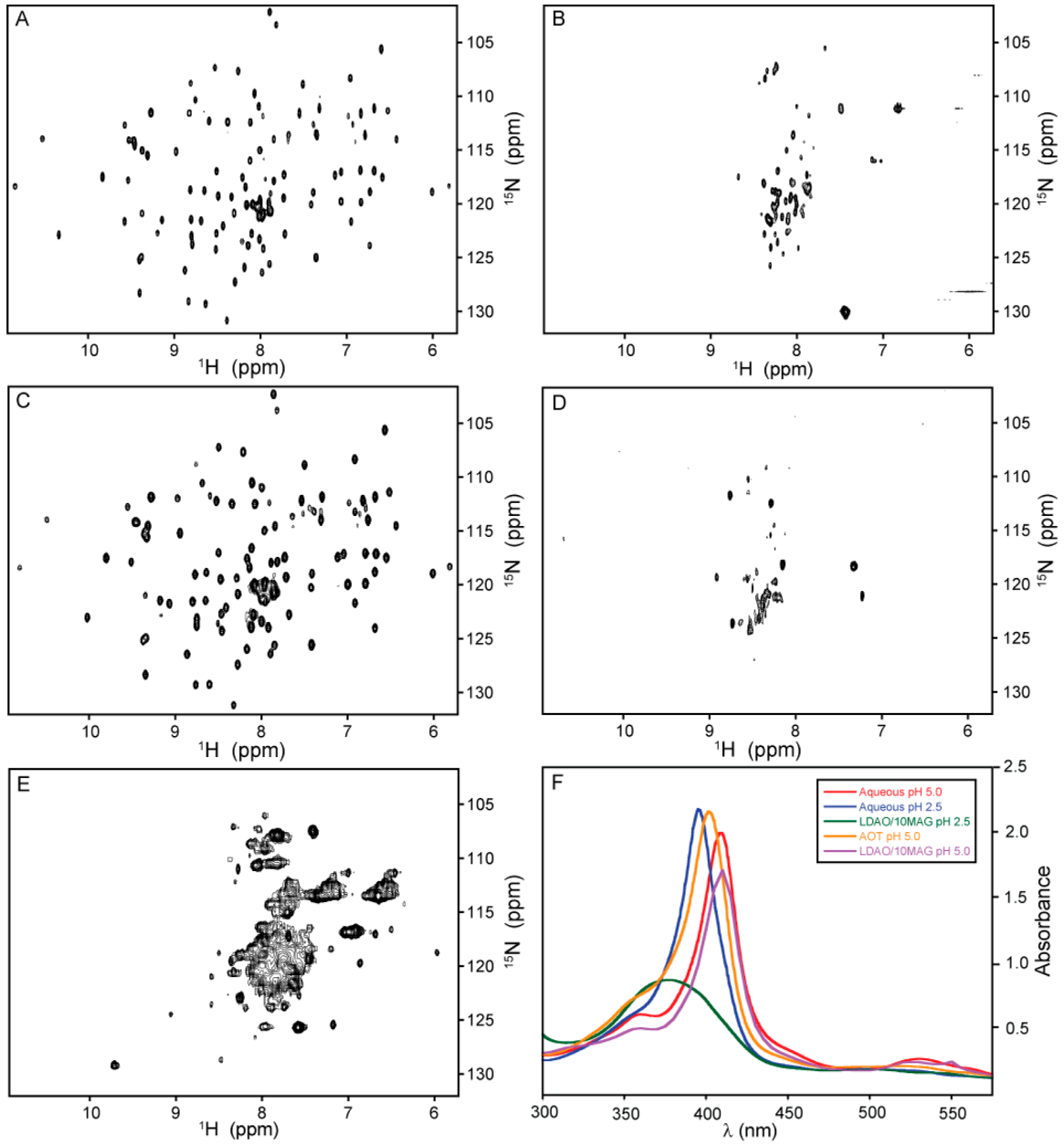

Figure 4. ^{15}N HSQC and Soret band absorption spectra of uniformly ^{15}N-labeled cytochrome *c* in aqueous solution at different pH and reverse micelle mixtures to monitor protein foldedness. Native aqueous cytochrome *c* at pH 5 (A) is shown to unfold at pH 2.5 in aqueous solution (B). Similarly, native RM-encapsulated cytochrome *c* in 10MAG/LDAO reverse micelle mixtures at pH 5 (C) is shown to unfold at pH ≈ 2.5 in the same mixture (D). Cytochrome *c* in AOT reverse micelles at pH 5 conversely is also unfolded (E). All reverse micelle mixtures had a final protein concentration of 140 μM and W_0 of 15. Normalized optical absorbance spectra of all samples (A–E) from 315 to 575 nm are also shown (F).

with great efficiency, but solution NMR measurements of these samples show that *most proteins are largely or completely unstructured in AOT reverse micelle solution*. Ubiquitin is the sole notable exception.[9,50−52] Figure 4 demonstrates the sensitivity of cytochrome *c* to the precise conditions of encapsulation. Though encapsulation in AOT reverse micelles solubilizes cytochrome *c*, a ^{15}N HSQC of the sample reveals that the protein is highly conformationally disordered, as evidenced by the collapsed spectrum (Figure 4E). The spectrum of aqueous cytochrome *c* conversely shows the typical dispersion of a stably folded protein (Figure 4A). Encapsulation of the protein in the charge-neutral 10MAG/LDAO surfactant mixture results in a sample with a spectrum that closely mimics that obtained in aqueous solution (Figure 4C). In this case, though the pH of the reverse micelle samples (as determined by the ^{1}H buffer signals) are identical to that in aqueous solution, the surfactants can significantly influence the structural state of the encapsulated protein. Using the buffer molecules as internal pH indicators, the unfolding of this protein as a function of pH can be reproduced in the 10MAG/LDAO reverse micelles with similar spectral results by NMR (Figure 4 B,D). Although some contribution from a denaturing interaction with the anionic headgroups of AOT is not ruled out, these results do point to an essential role for controlling the effective pH of the reverse micelle water core in maintaining the structural fidelity of the encapsulated protein.

Evaluation of these various conditions by visible absorption spectroscopy of the Soret band yields results that are much

dx.doi.org/10.1021/jp4103349 | J. Phys. Chem. B 2014, 118, 2020−2031

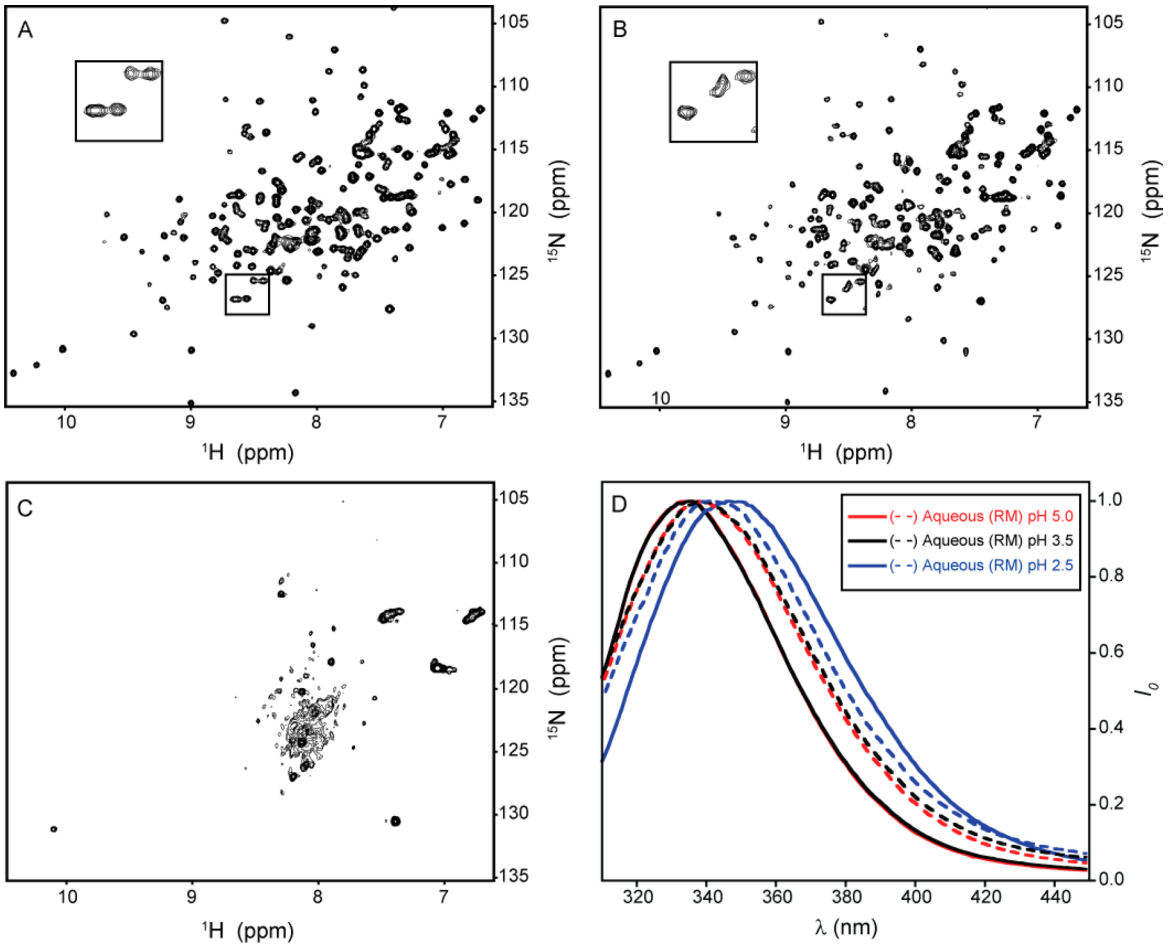

Figure 5. ^{15}N HSQC and fluorescence emission spectra of uniformily ^{15}N-labeled T4 lysozyme L99A mutant in reverse micelle mixtures at varying pH to monitor protein foldedness. Aqueous L99A mutant of T4 lysozyme at pH 5 is encapsulated in a natively folded state in a 10MAG/LDAO/DTAB reverse micelle mixture at a water loading of 18 (A). The pH of the sample was lowered to 3.5 to create a partially unfolded state (B) and subsequently lowered to pH 2.5 to create a fully unfolded state (C). Insets in (A) and (B) demonstrate protein unfolding by showing the collapse and disappearance of peaks. All reverse micelle mixtures had a final protein concentration of 80 μM. Tryptophan fluorescence emission spectra (D) of all three reverse micelle samples (A–C) along with aqueous samples at the same pH are shown in red, black, and blue, respectively. Solid lines represent the aqueous protein while dashed lines represent the reverse micelle mixture.

more difficult to interpret. The Soret absorption of the aqueous and 10MAG/LDAO-encapsulated proteins at pH 5 matches closely with absorbance maxima at 410 nm, but the absorption in AOT reverse micelles differs slightly. This difference has been noted previously and has been variously interpreted,[53−56] but the spectral change matches closely with that induced by unfolding of cytochrome *c* upon binding to DOPC micelles.[57] Note that the Q-band of the heme at ∼525 nm shows marked differences for the aqueous and 10MAG/LDAO-encapsulated protein despite the clear NMR evidence that both are in their native conformations. Though shift in the Q-band of the protein encapsulated in AOT is slight and therefore somewhat ambiguous, the NMR spectra clearly show that the protein is denatured in that reverse micelle system. The response of the Soret band to pH-induced unfolding of the protein[52] varies considerably between aqueous and reverse micelle conditions.

While the wavelength of maximal absorption shifts to 395 nm in aqueous solution at pH 2.5, the shift in 10MAG/LDAO reverse micelles is much more dramatic (375 nm). These data demonstrate the clarity offered by solution NMR and its necessity for evaluation of the structural integrity of encapsulated proteins as well as the utility of the present method for pH adjustment and monitoring in reverse micelle systems. The L99A mutant of lysozyme from T4 bacteriophage is also unfolded under acidic conditions. In aqueous solution, the protein is in a natively folded state at pH 5 and becomes increasingly unfolded as the pH is lowered until it is completely unfolded at a pH of 2.5 (Figure S1 of the Supporting Information). Figure 5 demonstrates that this is also the case for T4 lysozyme when encapsulated in the 10MAG/LDAO/DTAB reverse micelles. The encapsulated L99A mutant of T4 lysozyme is shown to maintain its native fold at a pH of 5 (5A). The pH was lowered by direct injection of HCl and monitored using the proton chemical shift of acetate buffer molecules. As the pH of the sample is lowered to 3.5, the ^{15}N HSQC spectrum (5B) shows that the protein is beginning to unfold. This is evident because of the collapse and disappearance of multiple peaks in the pH 3.5 spectrum as highlighted by the insets in Figures 5A and Figure 5B. Much like in aqueous solution, lowering the pH of the sample to 2.5 caused the loss and collapse of the majority of peaks in the ^{15}N HSQC spectrum (5C), indicating that the T4 lysozyme is fully unfolded.

Native tryptophan fluorescence is frequently used to assess the structural state of soluble proteins both in aqueous solution and in reverse micelles.[58] Figure 5D shows fluorescence spectra

dx.doi.org/10.1021/jp4103349 | J. Phys. Chem. B 2014, 118, 2020−2031

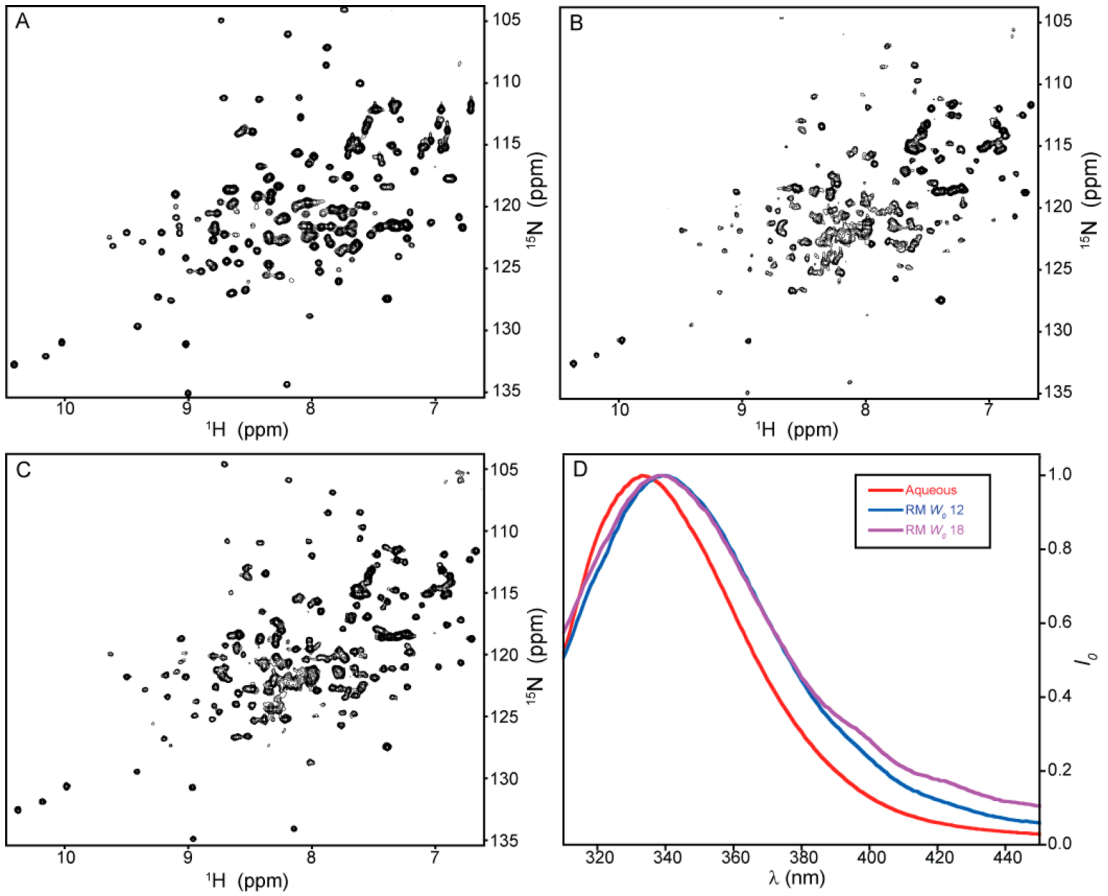

Figure 6. ^{15}N HSQC and fluorescence emission spectra of uniformly ^{15}N-labeled T4 lysozyme L99A mutant in aqueous solution and reverse micelle mixtures at various water loadings to monitor protein foldedness. Aqueous L99A mutant of T4 lysozyme at pH 5 (A) is encapsulated in a partially unfolded state in a 10MAG/LDAO/DTAB reverse micelle mixture at a water loading of 12. The water loading was increased to 18 (C) to allow for proper protein folding. Both reverse micelle mixtures had a final protein concentration of 80 μM. Tryptophan fluorescence emission spectra (D) of all three protein samples (A–C) are shown in red, blue, and purple, respectively.

of aqueous and encapsulated T4 lysozyme samples at pH 5, 3.5, and 2.5. Although the ^{15}N HSQC clearly demonstrates that the lysozyme is in a partially unfolded state at pH 3.5, the fluorescence spectra are virtually identical regardless of solution condition (bulk or RM). This could lead to incorrect assumptions about the protein's conformational state in the absence of NMR data. There is only a clear shift in the peak of the fluorescence emission from 339 to 342 nm (Figure 5D, blue dashed curve) once the protein is completely unfolded (Figure 5C) at pH 2.5. This phenomenon is replicated in aqueous solution (Figure 5D solid curves), although the shift in aqueous solution when the protein completely unfolds (from 334 to 348 nm) is much larger than in the reverse micelle mixture. These observations strongly suggest that solution NMR spectroscopy should be employed whenever possible to unambiguously assess the conformational state of encapsulated proteins.

In addition to the dependence of encapsulated proteins on the nature of the surfactant interface, the water content of the reverse micelle can also play an important role in maintenance of structural fidelity. Figure 6 shows the W_0 dependence of the L99A mutant of T4 lysozyme when encapsulated in 10MAG/LDAO/DTAB reverse micelles. The ^{15}N HSQC spectra of T4 lysozyme L99A clearly show that upon encapsulation of the aqueous protein (Figure 6A) in 10MAG/LDAO/DTAB reverse micelles, the amount of water within the reverse micelle ensemble greatly influences the protein conformational ensemble. At low W_0 many peaks that closely match the aqueous spectrum are observed, suggesting that the encapsulated protein is largely folded. However, the collapse and disappearance of a number of peaks show that the lysozyme populates a range of partially unfolded states under this condition (Figure 6B). Upon increasing the W_0 of the sample from 12 to 18, however, there is a marked improvement in spectral quality and the reappearance of the missing peaks indicating a shift toward a fully native fold (Figure 6C).

Native tryptophan fluorescence was used again to monitor the structural state of T4 lysozyme L99A mutant with varying W_0. Inspection of the tryptophan fluorescence spectra (Figure 6D) of the aqueous protein (red) upon encapsulation yields results that would be doubly misleading in the absence of NMR data. When encapsulated at a W_0 of 12 (blue), the native tryptophan fluorescence of T4 L99A shows a clear red shift of the emission peak maximum from 333 to 339 nm. Such a red shift is typically interpreted as being indicative of the exposure of tryptophan side chains to solvent due to protein unfolding. In the context of the reverse micelle, exposure to solvent becomes less straightforward to interpret than in aqueous solution. The ^{15}N HSQC of T4 L99A at W_0 of 12 (Figure 6B) shows clear resolution of three distinct tryptophan indole peaks (lower left of the spectrum) that closely match those in aqueous solution. The traditional interpretation of the fluorescence data argue that the tryptophan residues are in a

dx.doi.org/10.1021/jp4103349 | J. Phys. Chem. B 2014, 118, 2020–2031

non-native environment, but the NMR data clearly show that the tryptophan residues are largely in their native conformation. Upon increase of W_0 from 12 to 18, the fluorescence spectrum (purple) remains unchanged with the emission peak maximum remaining at 339 nm, despite the full structural fidelity evident in the NMR data at this condition. Here the fluorescence data alone would indicate that changing the W_0 had no impact on the encapsulated protein, but the NMR data clearly demonstrate that this is not the case. These data strongly indicate that NMR spectroscopy is optimal for both calibration of the internal pH of reverse micelle samples and confirmation of encapsulated protein structural fidelity.

■ ASSOCIATED CONTENT

Supporting Information

pH titration of T4 lysozyme L99A mutant in aqueous solution monitored with ^{15}N HSQC spectra. This material is available free of charge via the Internet at http://pubs.acs.org.

■ AUTHOR INFORMATION

Corresponding Author

*Telephone: 215-573-7288. Facsimile: 215-573-7290. E-mail: wand@mail.med.upenn.edu.

Author Contributions

†B.S.M. and N.V.N. contributed equally.

N.V.N., I.D., and A.J.W. designed the study. B.S.M., N.V.N., E.A.A., K.W.C.W., and I.D. performed the experiments and analyzed the data. The manuscript was written by B.S.M., N.V.N., and A.J.W. with editing contributions of all authors.

Notes

The authors declare the following competing financial interest(s): A.J.W. declares a competing financial interest as a Member of Daeadalus Innovations, a manufacturer of high pressure and reverse micelle NMR apparatus.

■ ACKNOWLEDGMENTS

We thank Kathleen Valentine, Sabrina Bédard, and Gurnimrat Sidhu for technical assistance in this work and Li Liang and Evan O'Brien for preparation of isotopically enriched ubiquitin and cytochrome *c*, respectively. This study was supported by NSF Grants MCB-0842814 and DMR05-200020, NIH Grant GM085120, NIH Postdoctoral Fellowship GM087099 to N.V.N., an NIH predoctoral training grant appointment to B.S.M. (GM071339), and a postdoctoral fellowship from the Swiss National Science Foundation to I.D.

■ ABBREVIATIONS

CTAB, cetyltrimethylammonium bromide; AOT, 75 mM bis(2-ethylhexyl)sulfosuccinate; LDAO, lauryldimethylamine oxide; 10MAG, decylmonoacylglycerol; DTAB, dodecyltrimethylammonium bromide; RM, reverse micelle

■ REFERENCES

(1) Correa, N. M.; Silber, J. J.; Riter, R. E.; Levinger, N. E. Nonaqueous Polar Solvents in Reverse Micelle Systems. *Chem. Rev.* **2012**, *112*, 4569−4602.

(2) Halle, B. Protein Hydration Dynamics in Solution: A Critical Survey. *Philos. Trans. R. Soc. London, Ser. B* **2004**, *359*, 1207−1223 (discussion 1223−1204, 1323−1208).

(3) Pal, S. K.; Zewail, A. H. Dynamics of Water in Biological Recognition. *Chem. Rev.* **2004**, *104*, 2099−2123.

(4) Mattea, C.; Qvist, J.; Halle, B. Dynamics at the Protein−Water Interface from O-17 Spin Relaxation in Deeply Supercooled Solutions. *Biophys. J.* **2008**, *95*, 2951−2963.

(5) Anarbaev, R. O.; Rogozina, A. L.; Lavrik, O. I. DNA Polymerase B Reveals Enhanced Activity and Processivity in Reverse Micelles. *Biophys. Chem.* **2009**, *141*, 11−20.

(6) De, T. K.; Maitra, A. Solution Behavior of Aerosol Ot in Nonpolar-Solvents. *Adv. Colloid Interface Sci.* **1995**, *59*, 95−193.

(7) Malik, A.; Kundu, J.; Mukherjee, S. K.; Chowdhury, P. K. Myoglobin Unfolding in Crowding and Confinement. *J. Phys. Chem. B* **2012**, *116*, 12895−12904.

(8) Saha, R.; Rakshit, S.; Verma, P. K.; Mitra, R. K.; Pal, S. K. Protein-Cofactor Binding and Ultrafast Electron Transfer in Riboflavin Binding Protein under the Spatial Confinement of Nanoscopic Reverse Micelles. *J. Mol. Recognit.* **2013**, *26*, 59−66.

(9) Babu, C. R.; Flynn, P. F.; Wand, A. J. Validation of Protein Structure from Preparations of Encapsulated Proteins Dissolved in Low Viscosity Fluids. *J. Am. Chem. Soc.* **2001**, *123*, 2691−2692.

(10) Kielec, J. M.; Valentine, K. G.; Babu, C. R.; Wand, A. J. Reverse Micelles in Integral Membrane Protein Structural Biology by Solution NMR Spectroscopy. *Structure* **2009**, *17*, 345−351.

(11) Valentine, K. G.; Peterson, R. W.; Saad, J. S.; Summers, M. F.; Xu, X.; Ames, J. B.; Wand, A. J. Reverse Micelle Encapsulation of Membrane-Anchored Proteins for Solution NMR Studies. *Structure* **2010**, *18*, 9−16.

(12) Van Horn, W. D.; Ogilvie, M. E.; Flynn, P. F. Use of Reverse Micelles in Membrane Protein Structural Biology. *J. Biomol. NMR* **2008**, *40*, 203−211.

(13) Babu, C. R.; Hilser, V. J.; Wand, A. J. Direct Access to the Cooperative Substructure of Proteins and the Protein Ensemble via Cold Denaturation. *Nat. Struct. Mol. Biol.* **2004**, *11*, 352−357.

(14) Pometun, M. S.; Peterson, R. W.; Babu, C. R.; Wand, A. J. Cold Denaturation of Encapsulated Ubiquitin. *J. Am. Chem. Soc.* **2006**, *128*, 10652−10653.

(15) Peterson, R. W.; Anbalagan, K.; Tommos, C.; Wand, A. J. Forced Folding and Structural Analysis of Metastable Proteins. *J. Am. Chem. Soc.* **2004**, *126*, 9498−9499.

(16) Van Horn, W. D.; Ogilvie, M. E.; Flynn, P. F. Reverse Micelle Encapsulation as a Model for Intracellular Crowding. *J. Am. Chem. Soc.* **2009**, *131*, 8030−8039.

(17) Luisi, P. L.; Giomini, M.; Pileni, M. P.; Robinson, B. H. Reverse Micelles as Hosts for Proteins and Small Molecules. *Biochim. Biophys. Acta* **1988**, *947*, 209−246.

(18) Workman, H.; Flynn, P. F. Stabilization of Rna Oligomers through Reverse Micelle Encapsulation. *J. Am. Chem. Soc.* **2009**, *131*, 3806−+.

(19) Narang, A. S.; Delmarre, D.; Gao, D. Stable Drug Encapsulation in Micelles and Microemulsions. *Int. J. Pharm.* **2007**, *345*, 9−25.

(20) Wand, A. J.; Ehrhardt, M. R.; Flynn, P. F. High-Resolution NMR of Encapsulated Proteins Dissolved in Low-Viscosity Fluids. *Proc. Natl. Acad. Sci. U.S.A.* **1998**, *95*, 15299−15302.

(21) Peterson, R. W.; Lefebvre, B. G.; Wand, A. J. High-Resolution NMR Studies of Encapsulated Proteins in Liquid Ethane. *J. Am. Chem. Soc.* **2005**, *127*, 10176−10177.

(22) Peterson, R. W.; Pometun, M. S.; Shi, Z. S.; Wand, A. J. Novel Surfactant Mixtures for NMR Spectroscopy of Encapsulated Proteins Dissolved in Low-Viscosity Fluids. *Protein Sci.* **2005**, *14*, 2919−2921.

(23) Dodevski, I.; Nucci, N. V.; Sidhu, G. K.; Valentine, K. G.; Wand, A. J. Optimized Reverse Micelle Surfactant System for High-Resolution NMR Spectroscopy of Encapsulated Proteins Dissolved in Low-Viscosity Fluids. *J. Am. Chem. Soc.* [Online early access]. DOI: 10.1021/ja410716w. Published Online: Feb 4, **2013**.

(24) Lefebvre, B. G.; Liu, W.; Peterson, R. W.; Valentine, K. G.; Wand, A. J. NMR Spectroscopy of Proteins Encapsulated in a Positively Charged Surfactant. *J. Magn. Reson.* **2005**, *175*, 158−162.

(25) Wand, A. J.; Urbauer, J. L.; McEvoy, R. P.; Bieber, R. J. Internal Dynamics of Human Ubiquitin Revealed by 13c-Relaxation Studies of Randomly Fractionally Labeled Protein. *Biochemistry* **1996**, *35*, 6116−6125.

(26) Hasegawa, M. Buffer-like Action in Water Pool of Aerosol Ot Reverse Micelles. *Langmuir* **2001**, *17*, 1426−1431.
(27) Crans, D. C.; Levinger, N. E. The Conundrum of pH in Water Nanodroplets: Sensing pH in Reverse Micelle Water Pools. *Acc. Chem. Res.* **2012**, *45*, 1637−1645.
(28) Elseoud, O. A.; Chinelatto, A. M.; Shimizu, M. R. Acid−Base Indicator Equilibria in the Presence of Aerosol-Ot Aggregates in Heptane—Ion-Exchange in Reversed Micelles. *J. Colloid Interface Sci.* **1982**, *88*, 420−427.
(29) Smith, R. E.; Luisi, P. L. Micellar Solubilization of Bio-Polymers in Hydrocarbon Solvents. 3. Empirical Definition of an Acidity Scale in Reverse Micelles. *Helv. Chim. Acta* **1980**, *63*, 2302−2311.
(30) Baruah, B.; Roden, J. M.; Sedgwick, M.; Correa, N. M.; Crans, D. C.; Levinger, N. E. When Is Water Not Water? Exploring Water Confined in Large Reverse Micelles Using a Highly Charged Inorganic Molecular Probe. *J. Am. Chem. Soc.* **2006**, *128*, 12758−12765.
(31) Baruah, B.; Crans, D. C.; Levinger, N. E. Simple Oxovanadates as Multiparameter Probes of Reverse Micelles. *Langmuir* **2007**, *23*, 6510−6518.
(32) Baruah, B.; Swafford, L. A.; Crans, D. C.; Levinger, N. E. Do Probe Molecules Influence Water in Confinement? *J. Phys. Chem. B* **2008**, *112*, 10158−10164.
(33) Sedgwick, M. A.; Crans, D. C.; Levinger, N. E. What Is inside a Nonionic Reverse Micelle? Probing the Interior of Igepal Reverse Micelles Using Decavanadate. *Langmuir* **2009**, *25*, 5496−5503.
(34) Fujii, H.; Kawai, T.; Nishikawa, H. Determination of pH in Reversed Micelles. *Bull. Chem. Soc. Jpn.* **1979**, *52*, 2051−2055.
(35) Halliday, N. A.; Peet, A. C.; Britton, M. M. Detection of pH in Microemulsions, without a Probe Molecule, Using Magnetic Resonance. *J. Phys. Chem. B* **2010**, *114*, 13745−13751.
(36) Vodolazkaya, N. A.; Mchedlov-Petrossyan, N. O.; Salamanova, N. V.; Surov, Y. N.; Doroshenko, A. O. Molecular Spectroscopy Studies of Solvent Properties of Dispersed "Water Pools" Fluorescein and 2,7-Dichlorofluorescein in Reversed Aot-Based Microemulsions. *J. Mol. Liq.* **2010**, *157*, 105−112.
(37) Fletcher, P. D. I.; Howe, A. M.; Robinson, B. H. The Kinetics of Solubilisate Exchange between Water Droplets of a Water-in-Oil Microemulsion. *J. Chem. Soc., Faraday Trans.* **1987**, *83*, 985−1006.
(38) Natarajan, U.; Handique, K.; Mehra, A.; Bellare, J. R.; Khilar, K. C. Ultrafine Metal Particle Formation in Reverse Micellar Systems: Effects of Intermicellar Exchange on the Formation of Particles. *Langmuir* **1996**, *12*, 2670−2678.
(39) Oldfield, C. Exchange Concept in Water-in-Oil Micro-emulsions—Consequences for Slow Chemical-Reactions. *J. Chem. Soc., Faraday Trans.* **1991**, *87*, 2607−2612.
(40) Tynkkynen, T.; Tiainen, M.; Soininen, P.; Laatikainen, R. From Proton Nuclear Magnetic Resonance Spectra to pH Assessment of ^{1}H NMR pH Indicator Compound Set for Deuterium Oxide Solutions. *Anal. Chim. Acta* **2009**, *648*, 105−112.
(41) Baryshnikova, O. K.; Williams, T. C.; Sykes, B. D. Internal pH Indicators for Biomolecular NMR. *J. Biomol. NMR* **2008**, *41*, 5−7.
(42) Alber, T.; Matthews, B. W. Structure and Thermal-Stability of Phage-T4 Lysozyme. *Methods Enzymol.* **1987**, *154*, 511−533.
(43) Muchmore, D. C.; Mcintosh, L. P.; Russell, C. B.; Anderson, D. E.; Dahlquist, F. W. Expression and N-15 Labeling of Proteins for Proton and N-15 Nuclear-Magnetic-Resonance. *Methods Enzymol.* **1989**, *177*, 44−73.
(44) Rumbley, J. N.; Hoang, L.; Englander, S. W. Recombinant Equine Cytochrome *c* in *Escherichia coli*: High-Level Expression, Characterization, and Folding and Assembly Mutants. *Biochemistry* **2002**, *41*, 13894−13901.
(45) Morcombe, C. R.; Zilm, K. W. Chemical Shift Referencing in MAS Solid State NMR. *J. Magn. Reson.* **2003**, *162*, 479−486.
(46) Gledhill, J. M.; Wand, A. J. Al NMR: A Novel NMR Data Processing Program Optimized for Sparse Sampling. *J. Biomol. NMR* **2012**, *52*, 79−89.
(47) Niemeyer, E. D.; Bright, F. V. The pH within Pfpe Reverse Micelles Formed in Supercritical CO_2. *J. Phys. Chem. B* **1998**, *102*, 1474−1478.
(48) Cavanagh, J. *Protein NMR Spectroscopy: Principles and Practice*, 2nd ed.; Academic Press: Boston, MA, 2007.
(49) Nucci, N. V.; Marques, B. S.; Bedard, S.; Dogan, J.; Gledhill, J. M., Jr.; Moorman, V. R.; Peterson, R. W.; Valentine, K. G.; Wand, A. L.; Wand, A. J. Optimization of NMR Spectroscopy of Encapsulated Proteins Dissolved in Low Viscosity Fluids. *J. Biomol. NMR* **2011**, *50*, 421−430.
(50) Ehrhardt, M. R.; Flynn, P. F.; Wand, A. J. Preparation of Encapsulated Proteins Dissolved in Low Viscosity Fluids. *J. Biomol. NMR* **1999**, *14*, 75−78.
(51) Wand, A. J.; Ehrhardt, M. R.; Flynn, P. F. High-Resolution NMR of Encapsulated Proteins Dissolved in Low-Viscosity Fluids. *Proc. Natl. Acad. Sci. U.S.A.* **1998**, *95*, 15299−15302. **1999**, *96*, 6571−6571.
(52) Goto, Y.; Calciano, L. J.; Fink, A. L. Acid-Induced Folding of Proteins. *Proc. Natl. Acad. Sci. U.S.A.* **1990**, *87*, 573−577.
(53) Chen, J.; Zhang, J. L.; Wu, Y. H.; Han, B. X.; Liu, D. X.; Li, Z. H.; Li, J. C.; Ai, X. H. Fluorescence Studies on the Microenvironments of Proteins in CO_2-Expanded Reverse Micellar Solutions. *J. Supercrit. Fluids* **2006**, *38*, 103−110.
(54) Gebicka, L. Peroxidase-like Activity of Cytochrome *c* in the Presence of Anionic Surfactants. *Res. Chem. Intermed.* **2001**, *27*, 717−723.
(55) Ono, T.; Goto, M. Peroxidative Catalytic Behavior of Cytochrome *c* Solubilized in Reverse Micelles. *Biochem. Eng. J.* **2006**, *28*, 156−160.
(56) Valdez, D.; Le Huerou, J. Y.; Gindre, M.; Urbach, W.; Waks, M. Hydration and Protein Folding in Water and in Reverse Micelles: Compressibility and Volume Changes. *Biophys. J.* **2001**, *80*, 2751−2760.
(57) Pinheiro, T. J.; Elove, G. A.; Watts, A.; Roder, H. Structural and Kinetic Description of Cytochrome *c* Unfolding Induced by the Interaction with Lipid Vesicles. *Biochemistry* **1997**, *36*, 13122−13132.
(58) Lakowicz, J. R. *Principles of Fluorescence Spectroscopy*, 3rd ed.; Springer: New York, 2006.